Towards an Empirically Based Parametric Explosion Spectral Model

S. R. Ford, W. R. Walter, S. Ruppert, E. Matzel, T. Hauk, R. Gok

October 7, 2009

Disclaimer

This document was prepared as an account of work sponsored by an agency of the United States government. Neither the United States government nor Lawrence Livermore National Security, LLC, nor any of their employees makes any warranty, expressed or implied, or assumes any legal liability or responsibility for the accuracy, completeness, or usefulness of any information, apparatus, product, or process disclosed, or represents that its use would not infringe privately owned rights. Reference herein to any specific commercial product, process, or service by trade name, trademark, manufacturer, or otherwise does not necessarily constitute or imply its endorsement, recommendation, or favoring by the United States government or Lawrence Livermore National Security, LLC. The views and opinions of authors expressed herein do not necessarily state or reflect those of the United States government or Lawrence Livermore National Security, LLC, and shall not be used for advertising or product endorsement purposes.

TOWARDS AN EMPIRICALLY BASED PARAMETRIC EXPLOSION SPECTRAL MODEL

Sean R. Ford, William R. Walter, Stan D. Ruppert, Eric Matzel, Terri F. Hauk, and Rengin Gok

Lawrence Livermore National Laboratory

ABSTRACT

Small underground nuclear explosions need to be confidently detected, identified, and characterized in regions of the world where they have never before been tested. The focus of our work is on the local and regional distances (< 2000 km) and phases (*Pn*, *Pg*, *Sn*, *Lg*) necessary to see small explosions. We are developing a parametric model of the nuclear explosion seismic source spectrum that is compatible with the earthquake-based geometrical spreading and attenuation models developed using the Magnitude Distance Amplitude Correction (MDAC) techniques (Walter and Taylor, 2002). The explosion parametric model will be particularly important in regions without any prior explosion data for calibration. The model is being developed using the available body of seismic data at local and regional distances for past nuclear explosions at foreign and domestic test sites. Parametric modeling is a simple and practical approach for widespread monitoring applications, prior to the capability to carry out fully deterministic modeling. The achievable goal of our parametric model development is to be able to predict observed local and regional distance seismic amplitudes for event identification and yield determination in regions with incomplete or no prior history of underground nuclear testing. The relationship between the parametric equations and the geologic and containment conditions will assist in our physical understanding of the nuclear explosion source.

OBJECTIVES

We aim to develop a practical explosion source parametric spectral model, based on all available data, that describes nuclear explosion *P*- and *S*-wave source spectra for a variety of geologic and containment conditions. This approach follows the simple earthquake parametric spectral model based on Brune (1970), which is used for the MDAC approach (Walter and Taylor, 2002) to improve earthquake/explosion discrimination. In regions without prior explosions, the parametric model could be combined with earthquake-derived path corrections to predict explosion regional phase amplitudes, improve discriminants such as *P/S* ratios, and support identification procedures (e.g., Event Classification Matrix, [ECM]) that explicitly need to use explosion discriminant probability density functions.

It is well known that depth and near-source material properties can affect seismic estimates of explosion yield, and prior work at the Nevada Test Site (NTS) (e.g., Walter et al., 1995) has found that explosions in weak materials have lower corner frequencies and steeper spectral fall-offs for *P*-waves than is predicted by the standard Mueller and Murphy (1971) model. As part of this research, we hope to quantify these effects as a function of frequency and wave type. Additionally, many of the most effective regional discriminants (high-frequency *P/S* ratios) make use of *S*-waves, as do *S*-wave coda yield estimation techniques, yet there remain many questions about how to predict explosion *S*-wave amplitudes. The development of a combined *P*- and *S*-wave spectral model consistent with observed regional *P*-and *S*-wave data is a goal of this work.
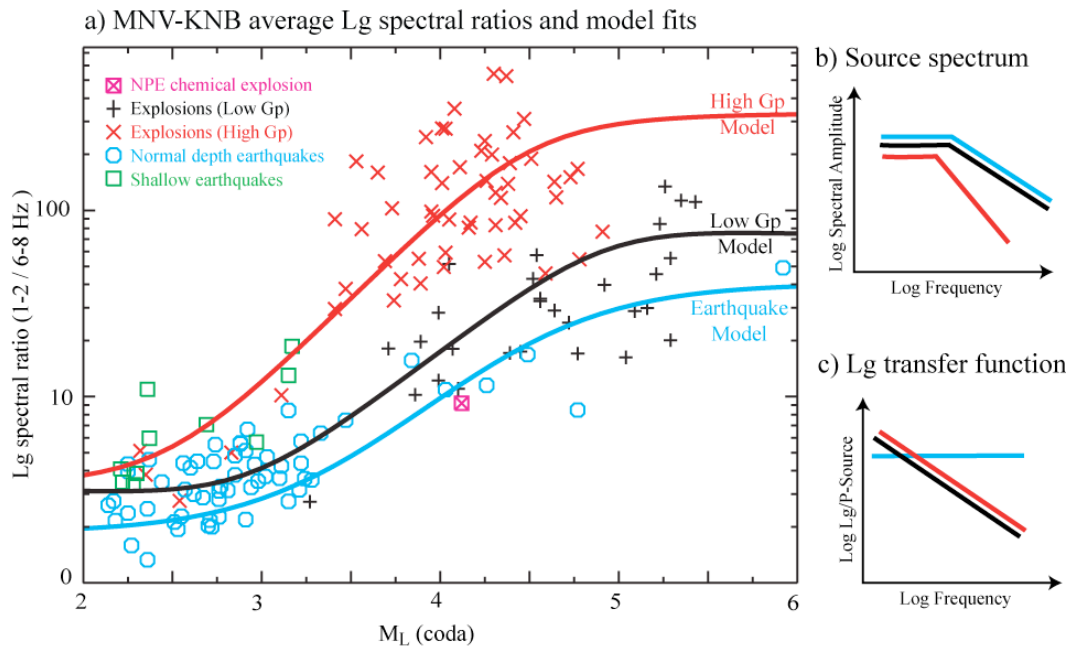

Figure 1. Simple first-order source model fits to low to high frequency spectral ratios of *Lg* amplitudes from Walter et al. (1995, Figure 8). Earthquake displacement spectra are fit with the Brune (1970) model (blue line), which is constant at low frequencies and falls off above a corner frequency as f^{-2}. Explosions are fit with two extremes of the Denny and Goodman (1990) model in order to investigate explosion dependence on emplacement material (namely, gas porosity [*Gp*]). The 'Low *Gp*' model (black line) has an effective fall-off similar to the earthquake model. The 'High *Gp*' model (red line) has a greater fall-off of f^{-3}.
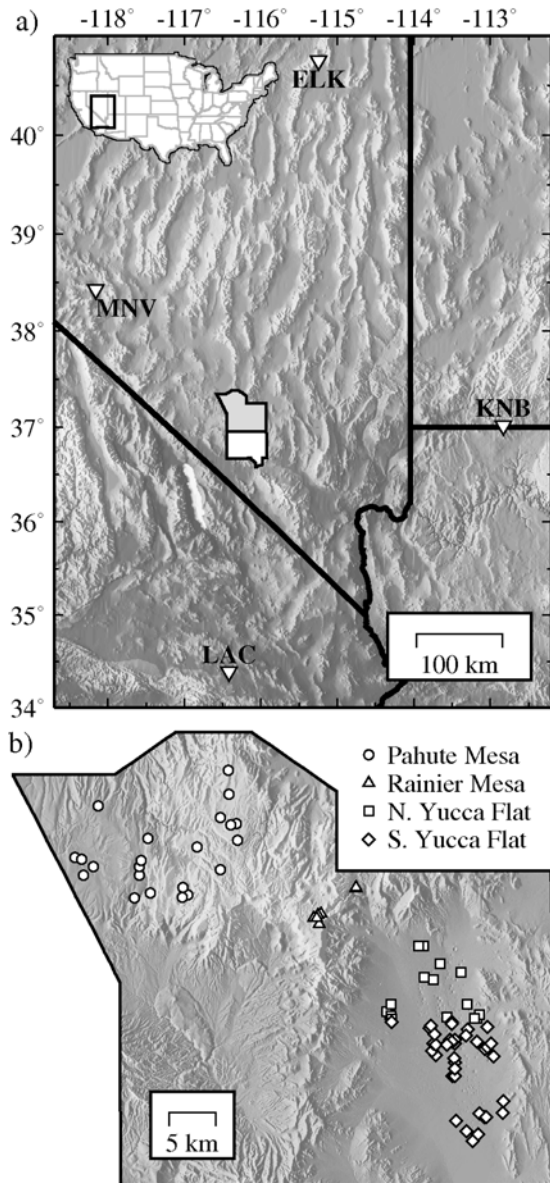
Introduction

Figure 2. a) Regional map of stations used in the analysis. The location of the map within the continental US is given by the inset map. The NTS is outlined and the shaded section is shown in (b). b) Map of the northern NTS with explosion locations and Vergino and Mensing (1990) area designations.

In previous work that looked at low to high frequency ratios of regional phase (e.g., *Pn*, *Pg*, *Lg*) amplitudes to separate explosions from earthquakes at NTS, Walter et al. (1995) noted that the results showed a strong dependence on the source media properties. Nuclear tests in weak and/or high gas porosity media tended to have higher values and discriminate better from earthquakes than explosions in stronger and/or lower gas porosity media. For example, in Figure 1 the ratio of the *Lg* amplitude at 1–2 Hz compared with the amplitude at 6–8 Hz is shown as a function of magnitude. The earthquakes (blue circles and green squares) show the expected trend with magnitude going from a low value for small events when the corner frequency is above 8 Hz and both measurements are on the constant part of the source spectra that is proportional to moment. For large magnitudes, the source corner frequency drops below 1 Hz and then both measures are on the part of the source spectra that decays with frequency as f^{-2}, resulting in high spectral ratio values. As magnitude increases, the earthquakes follow a sigmoid curve as shown by the blue line, which is based on the Brune (1970) model. The explosions are split into two categories based on the source media, a high gas porosity (*Gp*) and low strength group (red x) and low *Gp* high strength group (black crosses), and a clear difference between the two can be seen. In fact, the low *Gp* explosions reach spectral ratio values that imply much steeper falloff than f^{-2}.

To fit the explosion data we used two extremes of the Denny and Goodman explosion model (1990), which has two corner frequencies. In the low *Gp* case we allowed the second corner to be at a higher frequency than the range of interest, giving an effective f^{-2} falloff. In the high *Gp* case we forced the corners to be the same, giving an f^{-3} falloff. In both cases we used the observed 3 Hz corner frequency of the 1993 Non-Proliferation Experiment (NPE), a kiloton chemical explosion and assumed the corner frequency scales with the cube root of M_L(coda). Given that a pure explosion should not generate *S*-waves, one way to think about the *Lg* spectral ratio is as the product of the *P*-wave source ratio and a transfer function ratio, where the transfer function is a representation of how efficiently the source generated *P*-waves are converted (by whatever means) into *S*-waves. We estimated the transfer function ratio as a function of frequency as shown in Figure 1, and then multiplied the *P*-wave based Denny-Goodman model curves by these factors and then compared them to the *Lg* spectral ratio in Figure 1. The result is a fairly reasonable first order fit to the data. Interestingly since the explosion *Lg* transfer functions are larger than those for the earthquakes, it shifts the explosion *Lg* spectral ratios to relatively higher values than for the earthquakes, improving the discrimination performance of *Lg* spectral ratios over those of *Pn* alone (see Walter et al. 1995, Figure 7).

While in this case, the Denny and Goodman (1990) model provides a reasonable fit to these NTS data, it is not clear how we would make use of it in other regions. Furthermore the limitation of only two choices of high frequency falloff does not capture the full range of the observations. To develop a practical parametric source spectral model we want to be able to tie parameters like low frequency level, corner frequency and falloff rate to measureable properties like yield, depth, and media properties like gas porosity and strength. In the next section we take a more general approach to fitting the NTS explosion data. We focus first on *Pn* displacement spectra where previous work has shown that after correcting for path effects, the *Pn* spectra are a good representation of the source spectra (e.g., Goldstein et al., 1994). The initial goal is to develop a simplified *P*-wave explosion source model that matches the observed material property effects.

Data and methods

We employ the NTS explosion dataset of Walter et al. (2004), specifically the raw spectra of that dataset. Waveforms are de-meaned, de-trended and instrument corrected to acceleration. The signal is windowed with a 5% cosine taper that starts before the pick, where the time before the pick is 5% of the total time window. The Fourier transform is calculated and displacement spectra are obtained via double integration in the frequency domain. Finally, the resultant amplitude spectra are interpolated and smoothed to obtain a sampling period of $0.05 \log_{10}$ Hz.

Spectra for the *Pn* seismic phase for each explosion are calculated from the recordings of stations of the Livermore NTS Network, ELK (Elko, NV), KNB (Kanab, UT), LAC (Landers, CA), and MNV (Mina, NV). The locations of these stations relative to the NTS are given in Figure 2. These spectra are then corrected for geometrical spreading and regional, frequency-dependent attenuation of the form $Q = Q_0 f^{\gamma}$, where Q_0 is Q at 1 Hz and γ is the power-law dependence on frequency, f. We employ the Street et al. (1975) parametric form of geometrical spreading,

$$G(r) = \begin{cases} r^{-1}, & r < r_0 \\ 1/r_0\left(r_0/r\right)^{\eta}, & r \geq r_0 \end{cases}, \quad (1)$$

where r_0 is the distance at which the spreading transitions from spherical- to a cylindrical-type spreading and η is the distance dependence. The attenuation and spreading model parameters for each seismic phase are given in Table 1.
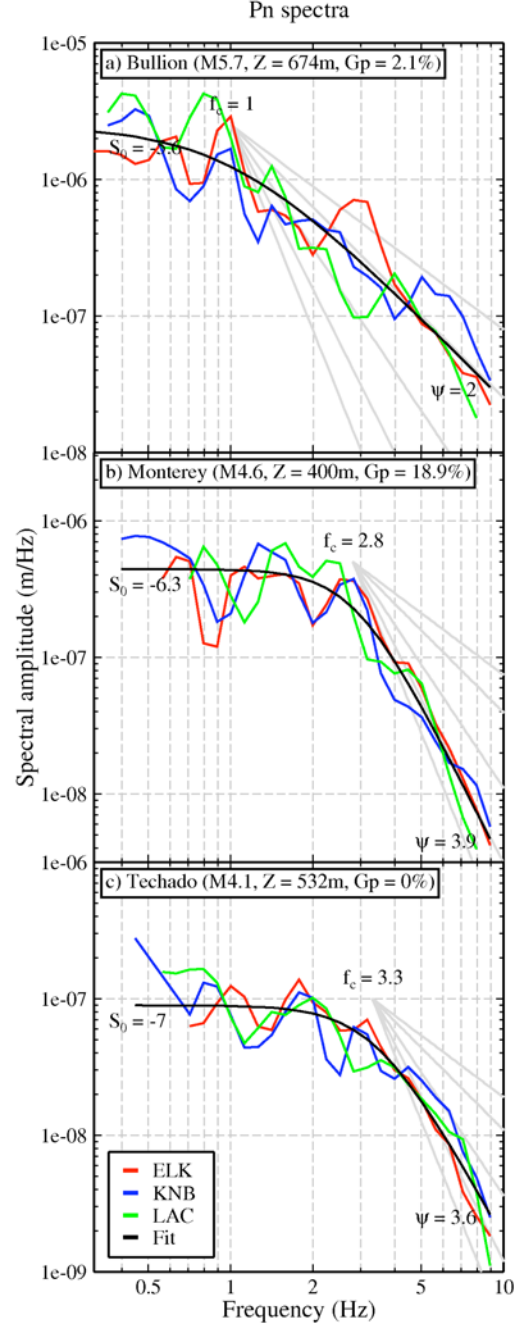

Figure 3. *Pn* spectra examples with the name, magnitude (where $M = m_b[Pn]$), depth (Z), and gas porosity (Gp) given in the subtitles. The long-period level (S_0), corner-frequency (f_c), and fall-off (ψ) are given in each plot, and the spectra are colored by station and the fit is shown in the legend in the lowermost plot. a) Spectra for an event with low *Gp* and ω^{-2} fall-off. b) Spectra for an event with high *Gp* and high fall-off. c) Spectra for an event with low *Gp* and high fall-off.

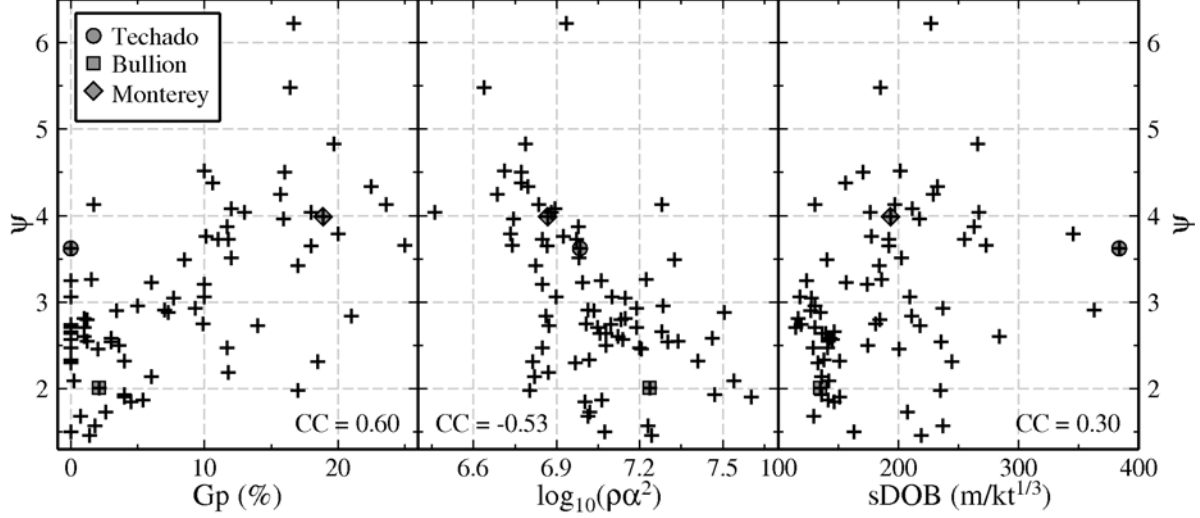**Figure 4.** ψ (spectral fall-off) comparison with geophysical parameters, a) gas porosity (*Gp*), b) the log-transform of strength ($\rho\alpha^2$), and c) sDOB = depth/$W^{1/3}$, where W is the yield estimated from $m_b(Pn)$. Correlation coefficients (CC) for each comparison are given at the bottom of the plot. Special symbols are given for events with spectra shown in Figure 3.

Table 1. Regional attenuation and geometric spreading parameters.

Phase	η	r_0 (km)	Q_0	γ
Pn	1.1	0. 001	210	0.65
Pg	0.5	100	190	0.45
Lg	0.5	100	200	0.54

In the future we will test path-specific attenuation parameters. In order for an event to enter the dataset, we require three of the four stations listed above to have recorded it with a signal-to-noise ratio greater than two. The maximum frequency considered is 9 Hz, since signal recorded above this frequency is often contaminated with non-stationary noise due to multi-band recording problems. In the future we will more systematically identify records with this problem and may be able to use higher frequencies for selected events. The spectra are jointly fit with a simple parametric form given by

$$S(f) = \frac{S_0}{1 + \left(f/f_c\right)^{\psi}}, \qquad (2)$$

Figure 5. *Pn* spectral fall-off (ψ) as a function of the log-transform of strength ($\rho\alpha^2$) and gas porosity (*Gp*). Small circles are colored according to ψ from the fit to Equation (2). Contours are for ψ as a planar fit to $\log_{10}(\rho\alpha^2)$ and *Gp* as described by Equation (3).

in a least-squares inversion that also provides standard error for each parameter estimate. Equation (2) describes the simplest behavior expected for seismic spectra. It has a constant level at low frequencies (S_0), which is proportional to static displacement, and falls off at high frequencies with a slope of $f^{-\psi}$ beyond a corner frequency f_c. Examples of the spectra and model fits are proportional to static displacement, and fall off at high frequencies with a slope of $f^{-\psi}$ beyond a corner frequency f_c. Examples of the spectra and model fits are
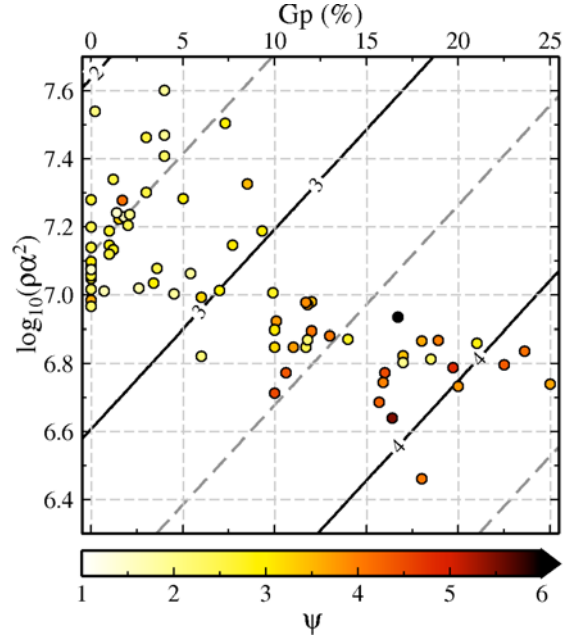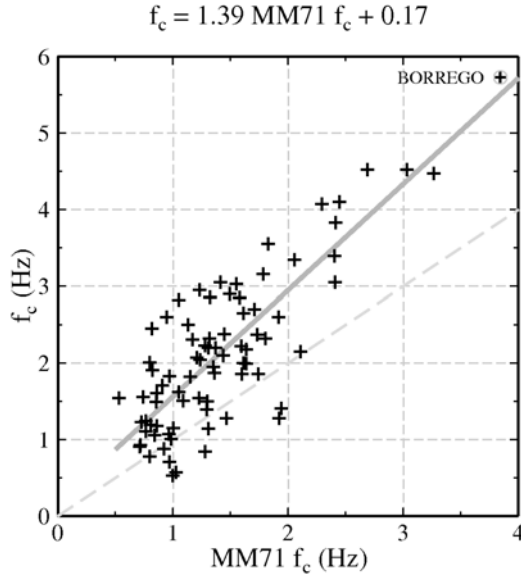
$$f_c = 1.39 \text{ MM71 } f_c + 0.17$$

Figure 6. **Corner-frequency (f_c) from the fits to Equation (2) compared with those predicted by Mueller and Murphy (1971), MM71 f_c. The linear relationship is given by the equation at the top of the plot and the slope is close to one.**

given in Figure 3. BULLION (Figure 3a) is fit well with a standard f^{-2} (ψ =2) spectral fall-off, but MONTEREY (Figure 3b), detonated in weak material, requires a steeper fall-off where the best fit $\psi \approx 4$. In the future, we will compare the model described by Equation (2) with other parametric models.

Preliminary results

We present the results of fitting the *Pn* spectra for NTS explosions in Figure 4. The spectral fall-off (ψ) correlates well with material properties such as gas porosity (Gp) and strength ($\rho\alpha^2$), where ρ is the density and α is the compressional velocity near the shot-point. There is less of a correlation with scaled depth-of-burial (sDOB = depth/yield$^{1/3}$). Yield was inferred from $m_b(Pn)$ based on the Vergino and Mensing (1990) relationship at NTS. sDOB can give insight to outliers in the ψ comparison with Gp and strength. For example, TECHADO (circle in Figure 4) has a very large sDOB and was detonated in a saturated *(Gp = 0%)* medium, but has a relatively high fall-off ($\psi = 3.6$, Figure 3c), a relationship that is different from the overall trend in the Gp data. Interestingly, TECHADO appears as less of an outlier in the fall-off versus strength plot (Figure 3b).

To quantitatively examine the relationship between spectral fall-off and material properties, we plot ψ versus $\log_{10}(\rho\alpha^2)$ and Gp and fit a plane to the data in Figure 5. The planar fit is weighted by the inverse variance of ψ. The spectral fall-off generally increases as strength decreases and Gp increases. The planar fit of the relationship between these material properties and fall-off is given by

$$\psi = 0.057Gp - 0.97\log_{10}(\rho\alpha^2) + 9.42 \,. \qquad (3)$$

As mentioned previously, sDOB has an effect on this relationship and will be investigated further in the future.

We present the best-fit f_c as a function of the corner frequency predicted by Mueller and Murphy (1971) as parameterized by Stevens and Day (1985) for tuff/rhyolite in Figure 6. The corner frequency in this study, f_c, is well-correlated with the Mueller and Murphy (1971) predicted corner-frequency and the slope is close to one. It can be made even closer by decreasing the reference elastic radius used to calculate the proportionality constant used in the Mueller and Murphy (1971) relationship. In the future, we will compare these results with those from *Lg* spectra to examine *S/P* corner frequency scaling in the context of variable spectral fall-off.

CONCLUSIONS AND RECOMMENDATIONS

Our preliminary analysis of *Pn* spectra of NTS explosions shows that a simple spectral model with variable fall-off is appropriate, and the fall-off correlates well with material properties. Corner-frequencies obtained with the variable fall-off model correlate with Mueller and Murphy (1971) corner-frequencies. If we use a smaller elastic radius than the one given for tuff, we believe we could match the trend of the Mueller-Murphy corner frequencies with a slope close to one.

Future work

This initial *P*-wave spectral fitting focused on correlating material properties with the model parameters. We will perform similar analyses for NTS seismic phases, *Pg* and *Lg*, and compare the results with those presented above for *Pn*. The comparison will allow for an examination of *P/S* scaling relationships, which can be compared with results from the Fisk (2007) study at NTS. The results of this study with a variable fall-off spectral model will be compared with other spectral models (e.g., Denny and Johnson [1991] and references therein). In addition, we will formally analyze the error and trade-offs in the estimated parameters of Equation (2). Finally, we will extend the analysis to other test sites to examine regional effects on the model parameters.

REFERENCES

Brune, J. N. (1970). Tectonic stress and the spectra of seismic shear waves from earthquakes, *J. Geophys. Res.* 75: 4997–5009.

Denny, M. D. and D. M. Goodman (1990). A case study of the seismic source function; SALMON and STERLING reevaluated, *J. Geophys. Res.* 95: 19705–19723.

Denny, M. D. and L. R. Johnson (1991). The explosion seismic source function: Models and scaling laws reviewed, in *Explosion Source Phenomenology*, eds. Taylor S. R. et al., AGU Monograph 65: 1–24.

Fisk, M. D. (2007). Corner frequency scaling of regional seismic phases for underground nuclear explosions at the Nevada Test Site, *Bull. Seis. Soc. Amer.* 97: 977–988.

Goldstein, P., S. P. Jarpe, K. M. Mayeda, and W. R. Walter (1994). Separation of source and propagation effects and regional distances, in *Proceedings of the Symposium on the Non-Proliferation Experiment: Results and Implications for Test Ban Treaties,* DOE-CONF-9404100, 6-272–6-276.

Mueller, C. S. and J. R. Murphy (1971). Seismic characteristics of underground nuclear detonations, Part I: Seismic spectrum scaling, *Bull. Seis. Soc. Amer.* 61: 1675–1692.

Stevens, J. L. and S. M. Day (1985). The physical basis of m_b:M_S and variable frequency magnitude methods for earthquake/explosion discrimination, *J. Geophys. Res.* 90: 3009–3020.

Street, R. L., R. B. Herrmann, and O. W. Nuttli (1975). Spectral characteristics of the Lg wave generated by central United States earthquakes, *Geophys. J. R. Astro.* 41: 51–63.

Vergino, E. S. and R. W. Mensing (1990). Yield estimation using regional mb(Pn), *Bull. Seis. Soc. Amer.* 80: 656–674.

Walter, W. R, K. D. Smith, J. L. O'Boyle, T. F. Hauk, F. Ryall, S. D. Ruppert, S. C. Myers, R. Abbot, and D. A. Dodge (2004). An assembled western United States dataset for regional seismic analysis, *Lawrence Livermore National Laboratory* , UCRL-TR-206630.

Walter, W. R. and S. R. Taylor (2002). A revised magnitude and distance amplitude correction (MDAC2) procedure for regional seismic discriminants, *Lawrence Livermore National Laboratory*, UCRL-ID-146882.

Walter, W. R., K. M. Mayeda, and H. J. Patton (1995). Phase and spectral ratio discrimination between NTS earthquakes and explosions, Part 1: Empirical observations, *Bull. Seis. Soc. Amer.* 85: 1050–1067.